Determining Atmospheric Density Using a Space-Launched Projectile

Gene P. Menees* and Chul Park*
NASA Ames Research Center, Moffett Field, California
John F. Wilson†
Informatics General Corporation, Palo Alto, California
and
Kevin G. Brown‡
NASA Ames Research Center, Moffett Field, California

A method that provides advance information about unpredictable atmospheric density dispersions that must be accommodated during random operations of aeroassisted orbital transfer vehicles (AOTVs) is proposed. The principal feature is that a test or "scout" projectile precedes the AOTV through the same region of the atmosphere as that of the predicted transatmospheric flight trajectory. The time lag between passage of the projectile and the AOTV can be adjusted to only that time necessary to implement required guidance, navigation, and control corrections. The various strategies available to control the projectile's flight characteristics are analyzed in detail. The results are correlated with aerothermodynamic heating and materials requirements to ensure the survival of the projectile and, consequently, the capability of the AOTV to navigate a variable upper atmosphere within specified limits.

Nomenclature

g = acceleration of gravity
H = altitude
I_p = specific impulse
L/D = lift-to-drag ratio
M = mass
$\dot{q}$ = convective heat flux
Q = total heat load over flight trajectory
r = projectile radius
R = range from target point (perigee of AOTV trajectory)
t = flight time from geosynchronous orbit
T = surface temperature
V = flight velocity
α = angle of attack
β = ballistic coefficient
γ = flight-path angle relative to local horizon
ΔR = range error
Δt = time interval (lead time) between arrival of projectile and AOTV at target point
ΔV = relative launch velocity between projectile and AOTV
$\Delta\gamma$ = relative launch angle between projectile and AOTV
λ = angular longitude at equator (equivalent to R)

Subscripts

f = rocket fuel
0 = launch time of projectile from AOTV
p = target point (perigee of AOTV trajectory)
P = projectile
s = stagnation point

Introduction

ONE of the principal design determinants of aeroassisted orbital transfer vehicles (AOTVs) is the ability to accommodate unpredictable dispersions in the density profile of the Earth's upper atmosphere. The magnitude of these random variations can approach ±50% in the altitude range within which AOTVs typically spend their operational lifetime (70-90 km).[1]

The dispersions in the atmospheric density and density shears of the type noted on recent Space Shuttle flights,[2] for example, present significant operational problems for AOTVs. The uncertainties in the aerodynamic characteristics can have a major effect on the vehicle performance [i.e., guidance, navigation, and control (GN&C) capabilities]. The development of adaptive guidance systems with verification of their capability to achieve desired terminal conditions will greatly increase the probability of success of spacebased AOTVs. However, this requires better information about the upper atmospheric structure, since guidance design considerations are directly affected. In addition to simplifying GN&C requirements, a better definition of the atmosphere provides many other payoffs. These include configuration weight optimization by reducing aerothermodynamic heating and aerodynamic loads, which is the principal factor determining the cost effectiveness (dollars per kilogram) of a given design and mission scenario.

The need to develop techniques to obtain data over the expected range of AOTV aeropass altitudes and locations is clearly a key technical issue. This is significant for all AOTV concepts, but especially so for the low lift-drag-ratio aerobrake-type designs that have been proposed for aeroassist flight demonstration tests. In almost two decades of space-tug/OTV conceptual studies, it has been shown that such designs provide superior performance as space freighters; however, the capability of these designs to navigate a variable upper atmosphere is an area of uncertainty.[3] The GN&C rationale is thus a crucial one for developing aerobraking AOTVs.

Design Philosophy

Several methods that have been proposed as means of attaining a better understanding of upper-atmosphere physics are illustrated in Fig. 1. These include Shuttle tether experiments; ground/airborne/satellite-based, laser Raleigh-backscatter surveys; and orbiter re-entry and flight development experiments. All of these techniques, however, are

Presented as Paper 85-0327 at the AIAA 23rd Aerospace Sciences Meeting, Reno, NV, Jan. 14-17, 1985; received March 25, 1985; revision received Aug. 7, 1985.

*Research Scientist. Member AIAA.
†Consultant, Professional Services Operations West.
‡Captain, USAF. Member AIAA.

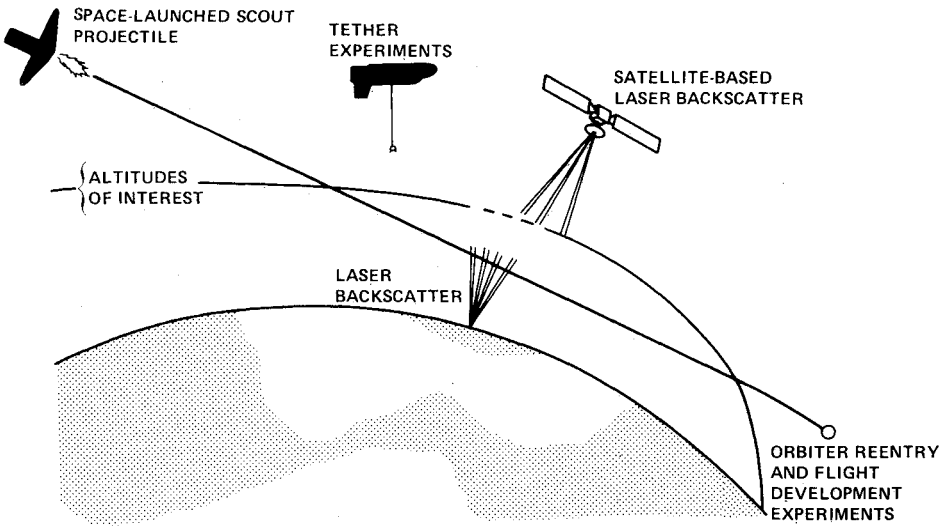

Fig. 1 Proposed methods for determining density distributions in the upper atmosphere.

limited to a narrow range of altitudes and locations that do not generally provide timely advance information about atmospheric conditions for random AOTV missions.

A new method is proposed that should substantially reduce these shortcomings. The essential feature is that a projectile is launched from the AOTV several minutes before its entry and along the predicted transatmospheric flight trajectory. The projectile acts as a "scout" that samples the atmospheric conditions shortly before the AOTV passes through the same region. It is proposed that the projectile's flight characteristics be monitored from autonomous radar or optical sensors on board the AOTV. Information about the atmospheric density structure may possibly be obtained from on-board processing of such data by the AOTV's computer facilities, with a real-time lag which is only of the order of that necessary to implement attitude changes of the AOTV to achieve required GN&C corrections.

There are at least three possibilities for propelling the scout projectile: explosive-charge (e.g., cartridges), electromagnetic-driven cannons (e.g., rail guns), and rocket launchers. Design details of the tracking and launching equipment are beyond the scope of this study. It is not expected, however, that the required mass and volume penalties would be excessive compared with typical AOTV entry masses, which are generally estimated to be at least 5000 kg for delivery-type missions and 10,000 kg for retrieval or abort missions. For example, portable rocket launchers for military applications are hand-carried and modern electronics allows micropackaging of sophisticated airborne radar systems.

Projectiles of the order of a few centimeters in diameter consisting of high-temperature materials appear to be most practical, because of their ability to withstand large heat-transfer rates. Much smaller meteoroid particles are routinely tracked from ground-based radar in the course of astronomical studies. In addition, a variety of geometries are possible (e.g., spheres, fin-stabilized missiles, blunted cones and cylinders). The design-optimized shape is a compromise of many tradeoffs between aerothermodynamic characteristics and surface materials requirements.

The general design philosophy for an innovative projectile proposed for this study is illustrated in Fig. 2. The shape approximates that of a flat disk in order to achieve some aerodynamic lift capability for imposed angles of attack. This provides additional flexibility to modulate the aeropass flight trajectories, as will be discussed subsequently. The approximate lift-to-drag ratio characteristics (Fig. 3) provide a substantial capability. Other design details include contouring the edges to alleviate the high concentrated edge heat fluxes and forming the geometry into a shell structure, which is a closer representation of the ideal flat plate. The flat surface is

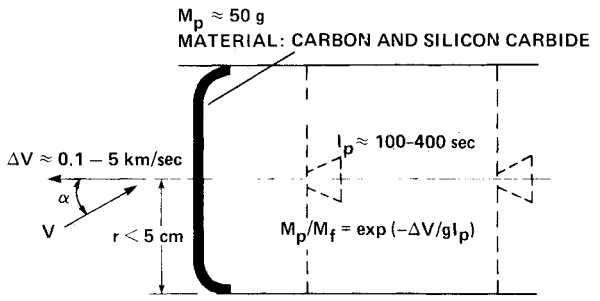

Fig. 2 General design philosophy of projectile and rocket launcher.

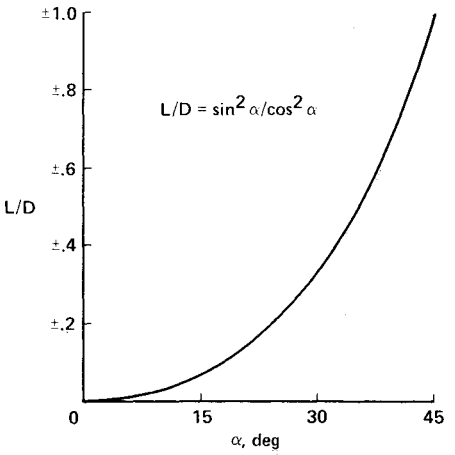

Fig. 3 Aerodynamic lift characteristics of a flat plate.

also beneficial in reducing the stagnation-point heat fluxes, since it provides a large effective nose radius. The projectile's shock-layer volume is still sufficiently small, however, that radiative heating is unimportant (since the average disk radius is only of the order of a few centimeters). In order to maintain preferred orientations relative to the flight path so as to achieve aerodynamic lift, the projectile will be spin-stabilized on launching from the AOTV in the same manner that a sounding rocket or satellite is stabilized. This imposes an invariant lift-to-drag ratio during the transatmospheric pass which, however, is a trivial constraint compared with the increased maneuverability that is obtained. The selection of construction materials is restricted by their heat-resistant characteristics to minimize mass-loss and shape-change effects for

optimal flight performance. All of these issues are discussed in greater detail below.

Results and Discussion

The example selected to illustrate application of the scout projectile is the return mission from geosynchronous orbit (GEO) of the conical lifting-brake AOTV design presented previously.[3-6] This vehicle has one of the lowest ballistic coefficients ($\beta = 11$ kg/m^2) of any proposed AOTV design and has the objective of achieving a very high perigee altitude to minimize design weight penalties incurred for the thermal protection system and for structural requirements. In addition, this case is of special interest because the location of a space station at GEO is expected to be an important future requirement; the mission scenario has received widespread analysis. Most of the present results were obtained for a projectile having a mass of 50g and a radius of 2.5 cm (≈ 1 in.), since these values are considered to provide a somewhat realistic upper limit for size and weight restrictions of the launch apparatus.

For example, the results shown in Fig. 4 indicate that a propellant mass of only about 0.5 kg (≈ 1 lb) is required to obtain a liberal upper limit on ΔV (5 km/s) relative to the AOTV's entry velocity (≈ 10 km/s) using a modest I_p of 200 s. These size and mass specifications provide a β of about 13.8 kg/m^2, which is near that of the AOTV. Calculations were obtained, however, for other values of β to determine its effect on the projectile's flight performance and aerothermodynamic heating characteristics. The ballistic coefficient is not a crucial factor in the application of the method, since it is one of several parameters that determine the projectile's operational flight envelope. The primary guideline in selecting values for β is to maintain surface heating effects below the level that produces significant changes in the magnitude of β (e.g., mass loss and shape change), within the constraints imposed by candidate construction materials.

Trajectory Analysis

A broad range of parametric studies has been made to demonstrate the basic feasibility of the concept. General details of the orbital change maneuver are shown in Fig. 5. The AOTV decircularizes from GEO with a retrothrust burn that produces an elliptical transfer orbit with perigee within the Earth's atmosphere. The AOTV's progress along the orbit is followed with various transit times indicated. In the interest of simplicity, the details of the aeroassist maneuver are not shown in Fig. 5. Aerobraking begins at about $H = 150$ km, however, and the perigee location or minimum altitude ($H \approx 86$ km) is reached at $t = 18{,}910$ s. The longitude is taken to be $\lambda = 0$ deg at GEO ($t = 0$ s); consequently, $\lambda = 180$ deg at perigee and aerobraking occurs near this range. The trajectory remains in a great circle plane, since the inclination change (28.5 deg) between GEO and the target orbit is obtained propulsively at GEO. The postaerobraking portion of the trajectory is also not shown in Fig. 5; however, it would have an apogee corresponding to a low Earth orbit (LEO) of about 450 km altitude where the AOTV would circularize and again achieve $\lambda = 0$ deg.[3]

Since the purpose of the scout projectile is to probe the atmospheric region through which the AOTV will transit, it must precede the AOTV's transatmospheric pass with sufficient lead time to allow the GN&C corrections that are required to accommodate unexpected dispersions. This is accomplished by specifying a target point in the atmosphere for the projectile's flight trajectory that is the exact perigee location of the AOTV's trajectory. During the AOTV's journey from GEO to its perigee the Earth rotates about 80 deg, which is an important factor in determining proper lead times and which must be accounted for in the projectile's launch conditions. The target point rotates with Earth, and its longitude is a function of time in inertial coordinates. The value of λ is 180 deg when the AOTV arrives, but is decreased by a predetermined amount that corresponds to the requirements of the projectile's flight. The difference between the arrival times of the projectile and AOTV is the desired lead time (Δt).

Extensive analysis of the orbital mechanics involved showed that there are only two regions, or "windows," along the AOTV's descent ellipse that are practical for launching the projectile. These locations are determined by the miss distance or range error (ΔR) that is obtained in reaching the target point for the possible launch conditions. The projectile's launch is characterized by three parameters relative to the AOTV's instantaneous values: the launch time (t_0), launch velocity (ΔV), and flight-path angle ($\Delta\gamma$). There are a variety of strategies and tradeoffs in the selection of appropriate launch conditions that are related to mission requirements and design capabilities. Most are generally excluded, however, because the projectile misses the target point by large distances as a consequence of the elliptical orbital equations. The projectile's true anomaly is determined after applying the launch parameters and is effectively its perigee longitude. This factor minus the target point's longitude is the range error (ΔR), which is a measure of the conformity of the projectile's flight path to that of the AOTV near perigee. The range errors and lead times associated with the launch parameters t_0 and ΔV for elliptical transfer orbits of the projectile are given in Fig. 6. The parameter $\Delta\gamma$ does not appear here but is used primarily to control the altitude error.

A principal feature of these results is that a narrow time slot (4000 s $< t_0 <$ 6000 s) occurs for zero range error or $\Delta R = 0$ (Figs. 5 and 6a). It is difficult to estimate the magnitude of acceptable errors for ΔR, since the extent of the atmospheric dispersions is not well known. An upper limit of the order of 100 km, however, would probably not be unreasonable. The results in Fig. 6a indicate that the launch window for this case corresponds to 4000 s $< t_0 <$ 9000 s, which is also shown in Fig. 5. The selection of appropriate launch conditions for t_0 and ΔV must be correlated with the associated Δt characteristics given in Fig. 6b. The objective is to achieve the lowest possible lead times that are consistent with GN&C requirements. This minimizes the Earth's rotational effects and decreases the probability of trajectories passing through the terminator where the cooling effects of sunrise and sunset become factors in the density variations.

The preceding discussion refers only to elliptical trajectories. It is possible to achieve a second launch window near the Earth with acceptable accuracy at the target point using an alternative strategy. This consists of launching the projectile at very late times and employing hyperbolic trajectories. These

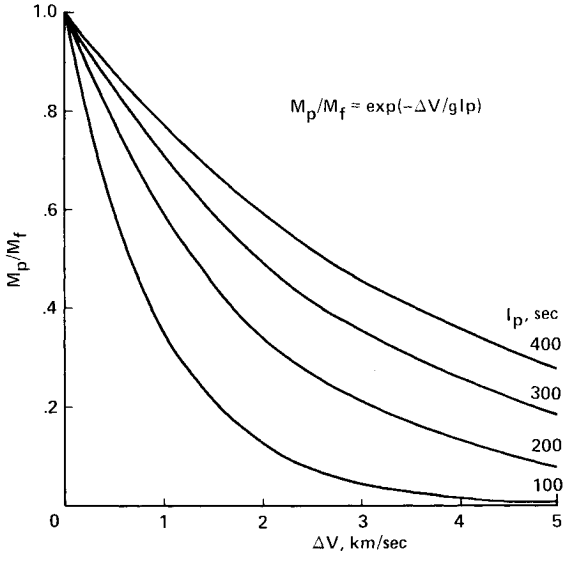

Fig. 4 Relative projectile-propellant mass requirements for various specific-impulse rocket launchers.

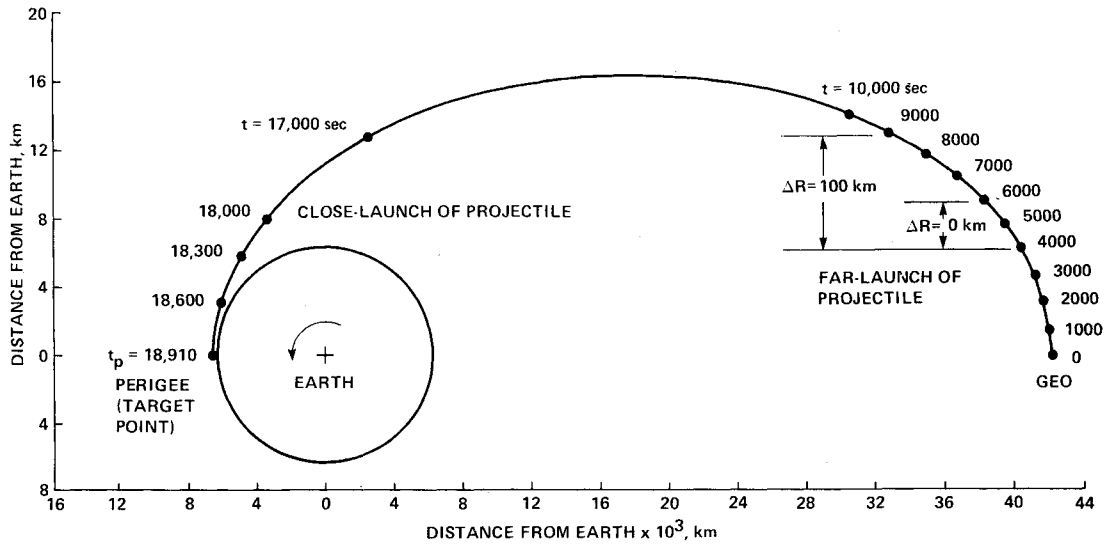

Fig. 5 AOTV elliptical descent trajectory from GEO.

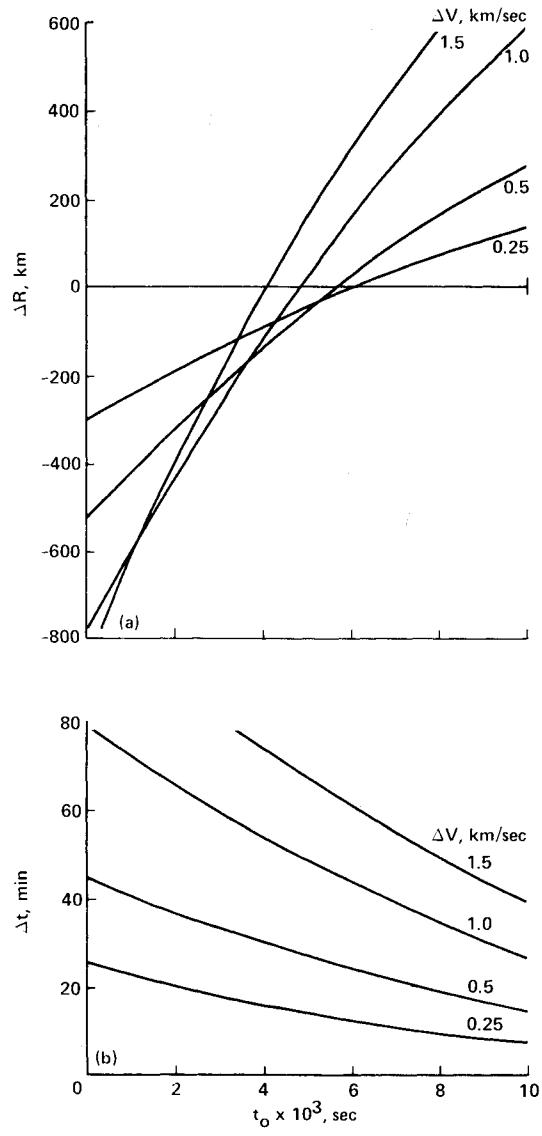

Fig. 6 Launch errors and lead times for elliptical descent orbits of projectile: a) range errors; b) lead times.

are essentially line-of-sight, straight-line hyperbolas of low eccentricity requiring large values of ΔV to obtain finite lead times. The $\Delta R - t_0$ analysis for this case is not shown; however, it is similar to, but more complicated than, that of the elliptical case. Consequently, there are two acceptable launch windows capable of achieving the specified ΔR of 100 km: 1) the "far launch," characterized by approximate values for the launch parameters of 4000 s $< t_0 <$ 9000 s, 0.25 km/s $< \Delta V <$ 1.5 km/s, and 8 min $< \Delta t <$ 80 min; and 2) the "close launch," characterized by 18,300 s $< t_0 <$ 18,910 s, 1 km/s $< \Delta V <$ 5 km/s, and 0 min $< \Delta t <$ 1 min.

Extensive trajectory analysis studies were performed for each launch window. Results for the close-launch case are discussed first, since it seemed logical initially to launch the projectile near the Earth. Representative results that span a broad range of entry parameters (see Table 1, cases 1-4) are given in Figs. 7 and 8. Projectile trajectories that correspond to the worst entry conditions ($\Delta V = 5$ km/s) and, therefore, highest surface heating rates of this study, are shown in Fig. 7. The two cases given are illustrative of the effect of negative lift in modulating the flight trajectories by raising the perigee locations. This is very beneficial in reducing the surface heating, as will be shown in the next subsection, but does not substantially affect Δt. The maximum value of Δt that could be obtained for this high-velocity launch was approximately 1 min, which required that the projectile be launched at $t_0 = 18{,}370$ s, or about 3 min $(t_p - t_0)$ before the AOTV's perigee. Launching at earlier times produces unacceptable errors in the range and altitude. For example, hyperbolic trajectories hit the Earth and elliptical trajectories miss most or all of the atmosphere.

Results for the approximate lower limit on ΔV of 1 km/s are given in Fig. 8. Two cases are shown that correspond to launch times about 5 and 10 min before the AOTV's perigee. The surface heating is substantially reduced because of the lower entry velocity; however, Δt is not significantly affected. There is, in fact, some gain in Δt for the 10-min case. The range error is outside the acceptable limit, however, because the AOTV is marginally beyond the straight-line distance for hyperbolic trajectories. Further decreases in ΔV require earlier launch times, but produce only incremental gains in Δt because of the small relative velocity of the projectile and AOTV at this stage of the descent orbit. The Δt value of about 1 min may be sufficient to implement GN&C corrections with automated control systems. If larger values are required, however, the far-launch window must be used.

Results that are representative of a far launch of the projectile (see Table 1, cases 5-7) are given in Fig. 9. The launch conditions ($t_0 = 6000$ s, $\Delta V = 0.5$ km/s, and $L/D = 0$) were selected to give a liberal lead time ($\Delta t = 24$ min). The transfer orbits are elliptical by necessity and, essentially, consist of rotating the AOTV's orbit slightly without changing its characteristics significantly. There are two problems associated with far launches that are more severe than they are with close launches. These are 1) the extreme aiming precision required because of the great travel distance involved, and 2) the tracking problems imposed by large lead times. For example, $\Delta t = 24$ min corresponds to a distance of about 12,000 km (7400 miles) near the Earth and may impose an impossible requirement for autonomous tracking systems. Values of Δt that are more of the order of a few minutes may be most realistic and can be obtained with a lower ΔV. Nevertheless, the present example illustrates the general principles involved for far-launched projectiles.

One method of solving the aiming problem is to use a cluster approach that consists of launching several scout projectiles to pass near the target point. This approach is illustrated in Fig. 9. Three cases are shown in which the launch parameters differ by only a slight spread in the flight-angle increment ($\Delta\gamma$). It is evident that this group of scouts would effectively cover the

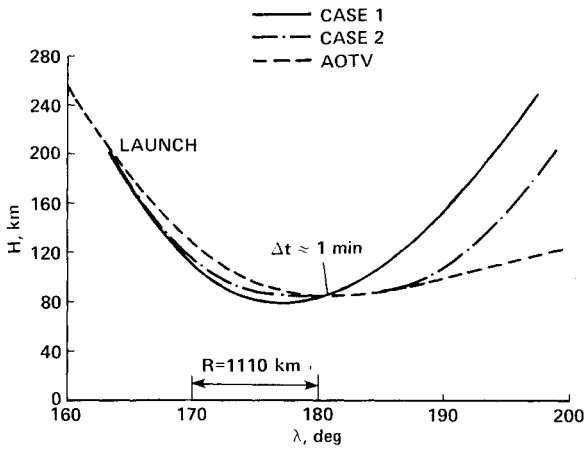

Fig. 7 Flight trajectories for close launch of projectile at $\Delta V = 5$ km/s ($t_p - t_0 = 3$ min).

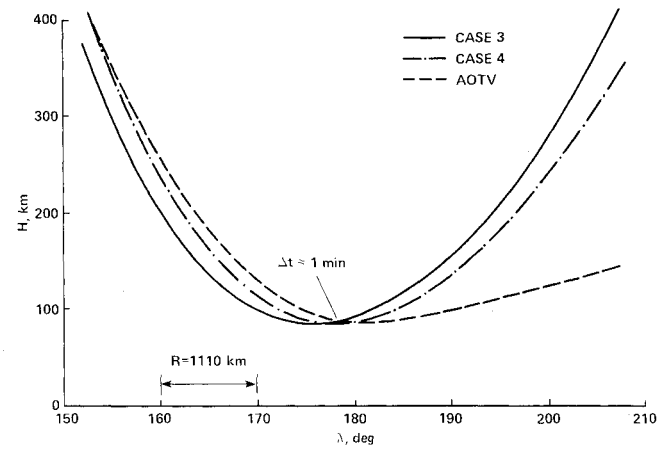

Fig. 8 Flight trajectories for close launch of projectile at $\Delta V = 1$ km/s ($t_p - t_0 = 5$ and 10 min).

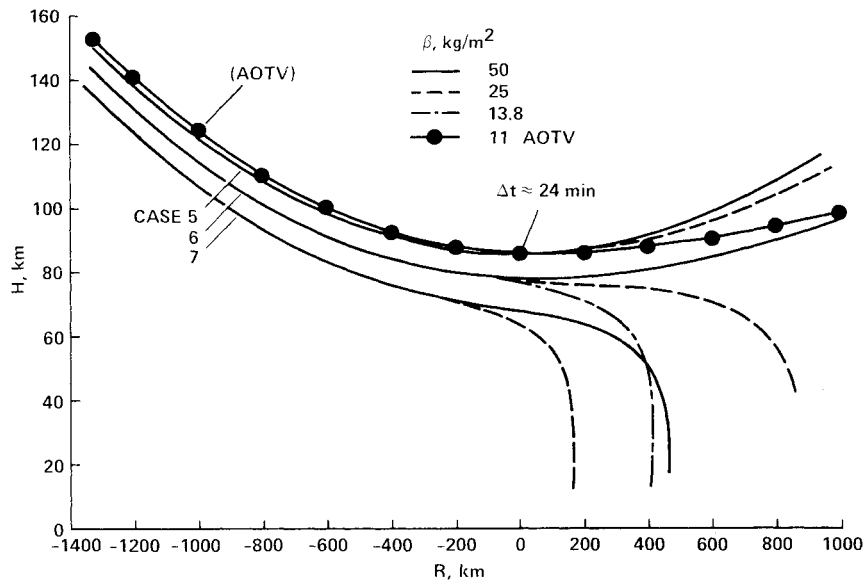

Fig. 9 Flight trajectories for far launch of projectile ($t_0 = 6000$ s, $\Delta V = 0.5$ km/s).

Table 1 Entry parameters

Case	t_0, s	$t_p - t_0$, min	ΔV km/s	$\Delta\gamma$, deg	β, kg/m²	L/D	Δt, min
Close launch							
1	18,730	3	5	−2.5	13.8	0	≈1
2	18,730	3	5	−2.09	13.8	−0.333	≈1
3	18,600	5	1	−1.3	13.8	0	≈1
4	18,300	10	1	−2.3	13.8	0	≈1
Far launch							
5	6,000	215	0.5	−10.634	25,50	0	≈24
6	6,000	215	0.5	−10.649	13,8,25,50	0	≈24
7	6,000	215	0.5	−10.664	25,50	0	≈24
AOTV (GEO)	0	–	–	–	11	0	–

space (range × altitude) and probe the density profile near the target point. The minute changes in the $\Delta\gamma$ requirements are not as formidable as they might appear. Analysis of the velocity-vector diagrams of the AOTV-scout projectile system shows that changes in the launch-thrust vector are much less sensitive than that of $\Delta\gamma$. Also shown in Fig. 9 is the effect of varying the ballistic coefficient (β) on the flight trajectories. For this example, the major influence occurs downrange of the target point and does not significantly affect the application of the cluster technique. In general, β affects the vehicle's deceleration and (mainly) the aerothermodynamic heating.

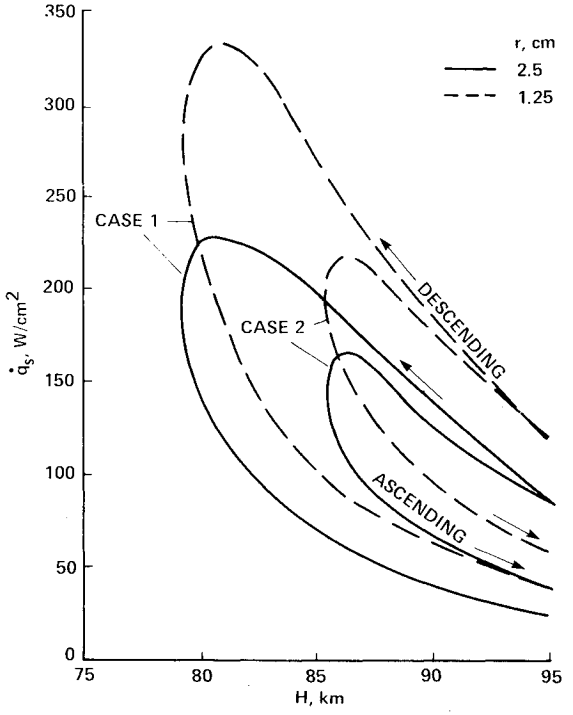

Fig. 10 Noncatalytic stagnation-point heat-transfer rates for close launch of projectile at $\Delta V = 5$ km/s ($T_W = 2500$ K).

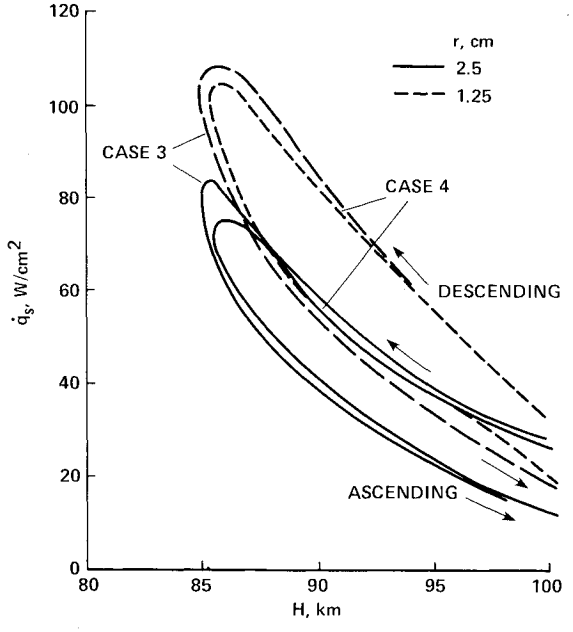

Fig. 11 Noncatalytic stagnation-point heat-transfer rates for close launch of projectile at $\Delta V = 1$ km/s ($T_W = 2500$ K).

Aerothermodynamic Heating

A major factor in the design of the scout projectile is the amount of heat transfer that it would experience during its flight through the atmosphere. The projectile should not burn up, and its size and weight must be negligible compared with that of the AOTV. In addition, mass loss and shape change should be minimal so that β remains nearly constant. The aerothermodynamic heating analysis of the projectile presents a unique problem in hypervelocity, rarefied-flow phenomena that has not been analyzed in detail. Extensive development work has been carried out for the present study and the details are presented in a companion paper.[7] Some of the principal features follow.

The total heat transfer experienced by a hypervelocity body is generally composed of both aerodynamic and radiative heating. Previous research, however, has shown that the radiative heating is negligible for small bodies in rarefied flow.[8,9] For the low-density flow conditions that are typical of this study, the postshock flow is in a state of thermochemical nonequilibrium. Consequently, the aerodynamic heating is composed of both conductive and diffusive heat transfer in which finite-rate relaxation effects are important for the chemical reactions. In addition, the low-density phenomena promote increased boundary-layer thickness, causing the boundary and shock layers to merge into a viscous layer. The combination of a body with small radius and high altitude classifies the flow in the "viscous-layer" regime over the region of highest heat transfer, which is near perigee. The traditional Rankine-Hugoniot relations for determining the postshock conditions become invalid for the viscous layer and must be modified to account for the viscous transport, that is, shock-slip conditions.[9] A nonequilibrium viscous shock-layer code was developed to account for the important physics of the flow phenomena. It is based on the one-dimensional shock-layer equations for stagnation-point flow,[10] with low-density effects properly accounted for, and is applicable to the free-molecular limit. For the present analysis, an ideal dissociating-gas model is assumed for air,[10,11] with properties that are based on the mass-weighted average values of oxygen and nitrogen. The reaction model is that of Kang,[12] and the reaction-rate coefficients are those of Park.[9]

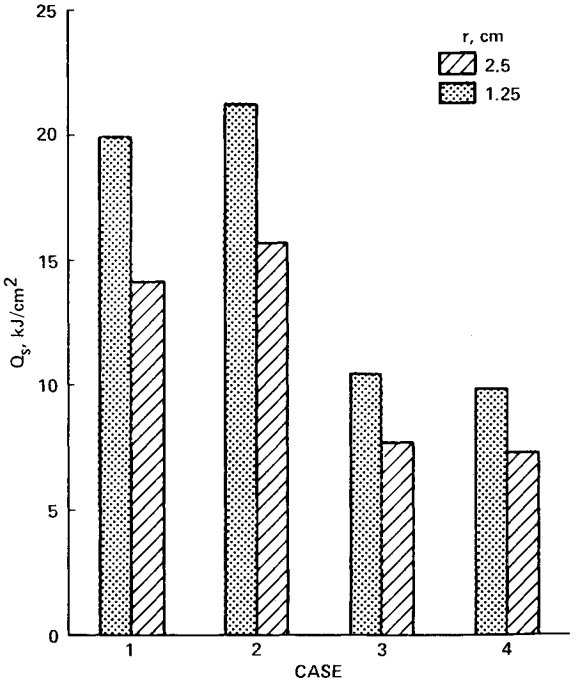

Fig. 12 Total stagnation-point heat loads over flight trajectories of projectile.

Results of the stagnation-point heat-transfer analysis are given in Figs. 10-13. Predictions were obtained for two representative sizes of projectiles that have disk radii of 1.25 and 2.5 cm. Surfaces are assumed to be noncatalytic to atom recombination for reasons that will be discussed in the next subsection, also to have a temperature of 2500 K. The heat-transfer calculations for the disk stagnation point are based on the "equivalent hemisphere" radius using the conversion given by Park.[13] The conversion factor is nearly 4 for the flight regimes of interest herein and provides equivalent nose radii of 5 and 10 cm, respectively, for the two projectiles.

The surface heat-flux distributions corresponding to the flight trajectories of the close-launch window (Table 1, cases 1-4) are given in Figs. 10 and 11. Maximum heating occurs near perigee for each trajectory because of the deceleration characteristics of the projectile, which maintains high velocity into the increasing density region of the perigee. The size of the projectile and the value of ΔV significantly impact the magnitude of the surface heating, as expected. In addition, the effect of negative lift (Fig. 10, case 2) in reducing the heat-transfer rates is clearly evident. The maximum value of $\dot{q}_s$ (370 W/cm^2) for the worst case considered (Fig. 10, case 1, $r = 1.25$ cm), however, is still below the level that requires ablating materials. Results are not given for the far-launch window, since the entry velocity is the lowest considered in this study. The total integrated heat load over the flight trajectories is also an important design parameter, and the results are presented in Fig. 12. Although case 1 has the highest heat fluxes, the largest values occur for case 2, because of the longer duration of the atmospheric pass resulting from negative lift.

It is important to emphasize that the present heat-transfer code has some limitations for application to low-density flow. The freestream Reynolds number based on the equivalent hemispherical nose radius of the projectile is a convenient correlating parameter. The results are considered good above a Reynolds number of about 300, but deteriorate below this value because the equations accounting for the shock-slip conditions become unstable and difficult to solve. This limit translates to an altitude of about 90 km for the small body and about 95 km for the large body. Consequently, the heat-transfer predictions above these altitudes are extrapolations toward the free-molecular-flow values. The results presented for this study are, therefore, mostly valid since the bulk of the heating occurs near the trajectory perigee locations, which have altitudes less than 85 km.

Materials Analysis

The aerothermodynamic heating predictions show that the front face of the scout projectile will experience large heat-transfer rates. A major design objective is to achieve minimal loss of material so that β remains nearly constant over the flight trajectories. A screening analysis of candidate high-temperature construction materials shows that the design requirements are currently best satisfied by silicon carbide in the nose-cap region. The high-temperature capability of this material has been proven for the Space Shuttle flights.[14] The nose-cap and leading-edge regions of the Shuttle consist of advanced carbon-carbon panels that are coated with silicon carbide and further overcoated with glass formers to prevent cracking. This system, which is called a reaction cured glass (RCG) coating, ensures temperatures to nearly 2000 K with minimal material loss through vaporization. Operational temperatures, however, are restricted to less than 2000 K, since the Shuttle is reusable. In addition, silicon carbide has another important characteristic that is a principal reason for its selection; the surface has nearly noncatalytic properties to atom recombination for the RCG coating used on the Shuttle.[15] This feature was incorporated into the previous aerothermodynamic heating predictions.

Results for the total mass lost by the projectile for the surface heat-transfer predictions corresponding to the close-launch window are given in Fig. 13. The calculations were obtained assuming free evaporation at the equilibrium radiation temperature for full accommodation of the surface heat flux at each point in the trajectory. The surface emissivity was assumed to be 0.8 and the evaporation rate was determined from Ref. 16 for all cases. Realistically, the vaporization process is not of the free type over the bulk of the flight trajectories. The stagnation-point pressure can exceed the vapor pressure by as much as three orders of magnitude in the region of peak heating near perigee. In such an environment, material loss rate is dictated mostly by the rate of diffusion of the vapor, that is, a diffusion-controlled regime exists. Consequently, corrections were applied where appropriate that restricted the evaporation rate to diffusion-limited values based on the work of Ref. 17. The general conclusion obtained from Fig. 13 is that the mass loss is not significant, even for the worst heating conditions (case 1), compared with the proposed total mass for the projectile. These results imply that the scout projectile concept is applicable to a much broader range of AOTV trajectories than the single case analyzed herein. Considerably more mass loss could be tolerated before there would be significant changes in β. Future research in materials technology will further extend the scout projectile's application. For example, a new thermal protection material under development at NASA agencies [fibrous-reusable-ceramic insulation (FRCI)] should be availabe within two years; it will extend the surface temperature capability substantially.

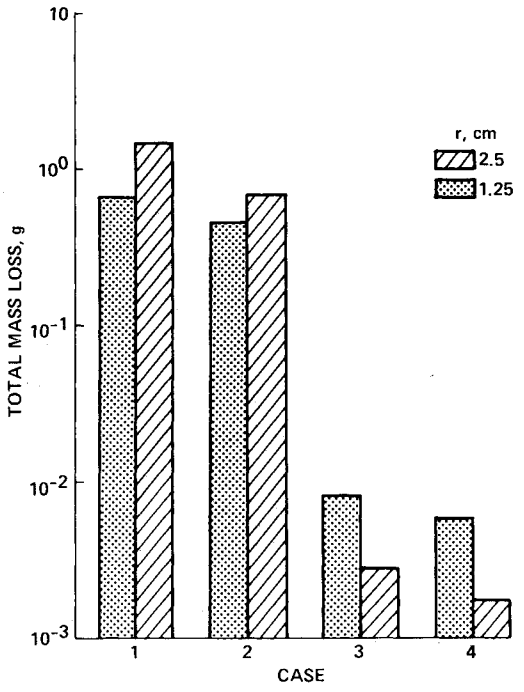

Fig. 13 Total mass loss over flight trajectories of projectile.

Concluding Remarks

A new method has been proposed for obtaining advance information about the unpredictable atmospheric density dispersions that must be accommodated during random operations of AOTVs. The unique feature is that a projectile is launched from the AOTV before its entry and probes the atmosphere in the same region through which the AOTV will travel. Extensive analysis of the launch and trajectory requirements was made to identify favorable operational characteristics. Correlations with aerothermodynamic heating and candidate construction materials were obtained to minimize mass-loss and shape-change effects on flight parameters. In general, the results show the fundamental feasibility of the method. Optimal application is probably to

the coplanar-type trajectories obtained with aerobrake AOTV designs, because of the projectile's moderate lifting capability. Further analysis of the lateral-turn, cross-range trajectories that are characteristic of high-lift, aeromaneuvering AOTV designs is needed. In addition, a comprehensive design analysis of the projectile, launching equipment, and tracking system is needed, because of the exploratory nature of this study.

References

[1]Walberg, G. D., "A Review of Aeroassisted Orbital Transfer," *Journal of Spacecraft and Rockets,* Vol. 22, March-April 1985, pp. 3-18.

[2]Findlay, J. T., Kelly, G. M., and Troutman, P. A., "Final Report—Shuttle Derived Atomspheric Density Model (Parts 1 and 2)," NASA CR 171824, Dec. 1984.

[3]Menees, G. P., Park, C., and Wilson, J. F., "Design and Performance Analysis of a Conical-Aerobrake Orbital-Transfer Vehicle Concept," *Thermal Design of Aeroassisted Orbital Transfer Vehicles,* edited by H. F. Nelson, Vol. 96, Progress in Astronautics and Aeronautics, AIAA, New York, 1984, pp. 286-308.

[4]Davies, C. B. and Park, C., "Aerodynamic Characteristics of Generalized Bent Biconic Bodies for Aeroassisted, Orbital-Transfer Vehicles," *Journal of Spacecraft and Rockets,* Vol. 22, March-April 1985, pp. 104-111.

[5]Menees, G. P., "Thermal-Protection Requirements for Near-Earth Aeroassisted Orbital-Transfer Vehicle Missions," *Thermal Design of Aeroassisted Orbital Transfer Vehicles,* edited by H. F. Nelson, Vol. 96, Progress in Astronautics and Aeronautics, AIAA, New York, 1984, pp. 257-285.

[6]Menees, G. P., Davies, C. B., Wilson, J. F., and Brown, K. G., "Aerothermodynamic Heating Analysis of Aerobraking and Aeromaneuvering Orbital Transfer Vehicles," *Thermal Design of Aeroassisted Obital Transfer Vehicles,* edited by H. F. Nelson, Vol. 96, Progress in Astronautics and Aeronautics, AIAA, New York, 1984, pp. 338-360.

[7]Brown, K. G., "Chemical and Thermal Nonequilibrium Heat Transfer Analysis for Hypervelocity, Low Reynolds Number Flow," AIAA Paper 85-1033, June 1985.

[8]Anderson, J. D. Jr., "An Engineering Survey of Radiating Shock Layers," *AIAA Journal,* Vol. 7, Sept. 1969, pp. 1666-1675.

[9]Park, C., "Problems of Rate Chemistry in the Flight Regimes of Aeroassisted Orbital Transfer Vehicles," *Thermal Design of Aeroassisted Orbital Transfer Vehicles,* edited by H. F. Nelson, Vol. 96, Progress in Astronautics and Aeronautics, AIAA, New York, 1984, pp. 511-537.

[10]Park, C., "Dissociative Relaxation in Viscous Hypersonic Shock Layers," *AIAA Journal,* Vol. 2, July 1964, pp. 1202-1207.

[11]Chung, P. M., "Hypersonic Viscous Shock Layer of Nonequilibrium Dissociating Gas," NASA TR R-109, 1961.

[12]Kang, S. W., "Nonequilibrium, Ionized, Hypersonic Flow Over a Blunt Body at Low Reynolds Number," *AIAA Journal,* Vol. 8, July 1970, pp. 1263-1270.

[13]Park, C., "Calculation of Radiation from Argon Shock Layers," *Journal of Quantitative Spectroscopy and Radiative Heat Transfer,* Vol. 28, Jan. 1982, pp. 29-40.

[14]Curry, D. M., Lathcem, J. W., and Whisehunt, G. B., "Space Shuttle Leading Edge Structural Subsystem Development," AIAA Paper 83-0483, Jan. 1983.

[15]Scott, C. D., "Effects of Nonequilibrium and Catalysis on Shuttle Heat Transfer," submitted to the *Journal of Spacecraft and Rockets.*

[16]Hirth, J. P. and Pound, G. M., "Condensation and Evaporation," *Progress in Materials Science,* Vol. 11, 1963, p. 1.

[17]Metzer, J. W., Engel, M. J., and Diaconis, N. S., "Oxidation and Sublimation of Graphite in Simulated Re-entry Environments," *AIAA Journal,* Vol. 5, March 1967, pp. 451-460.